

## Morphing wing design via aeroelastic tailoring

J. Enrique Herencia<sup>1</sup>, Paul M. Weaver<sup>2</sup> and Michael I. Friswell<sup>3</sup>  
*University of Bristol, Bristol BS8 1TR, UK*

An approach to design an aircraft wing with morphing capabilities employing aeroelastic tailoring is presented. Morphing capabilities are achieved by passive actuation, that is the aircraft wing will adapt itself to improve its performance during the designed flight conditions. The approach consists of an aeroelastic steady-state scheme with aero-structure coupling embedded within a global optimisation. The global optimisation is divided into two levels. At the first level, Mathematical Programming (MP) is used to optimise the wing under structural and aerodynamic constraints. Wing-box panels (skins and spars) are modelled using lamination parameters accounting for their anisotropy. Panels are assumed to be symmetric or mid-plane symmetric laminates with 0, 90, 45 or -45 degree ply angles. Each of the wing-box panels is subjected to a combined in-plane loading under strength, buckling and practical design constraints. At the second level, the actual lay-ups of the wing-box panels are obtained using a Genetic Algorithm (GA), accounting for manufacture and design practices.

### Nomenclature

$a$	=	panel length
$A$	=	membrane stiffness matrix, membrane
$A_{ij}$	=	terms of the membrane stiffness matrix, $i=j=1,2,6$
$A_{skin}^i$	=	area of the skin for the $i$ th panel
$A_{spar}^i$	=	area of the spar for the $i$ th panel
$b^i$	=	width of the $i$ th skin panel
$bs$	=	wing semi-span
$c$	=	wing chord, continuous
$C$	=	compression
$d$	=	discrete
$D$	=	bending stiffness matrix, bending, induced drag
$D_{ij}$	=	terms of the bending stiffness matrix, $i=j=1,2,6$
$E_{ij}$	=	Young's modulus in $ij$ direction, $i=j=1,2$
$G_{ij}$	=	shear modulus $i=1, j=2$
$G_i$	=	$i$ th design constraint
$h_i$	=	laminate thickness of the $i$ th panel
$h_w^i$	=	height of the $i$ th spar panel
$L$	=	lift
$M$	=	mass of the wing-box structure, running moment vector
MS	=	mid-plane symmetric
RBN	=	rib bay number
$N, \vec{N}$	=	running load vector, internal loads
$N_i$	=	load per unit length in $i$ direction, $i=x,y,xy$
$N_i^{cr}$	=	critical buckling load per unit length, $i= x,y,xy$

<sup>1</sup> Marie Curie Research Assistant, Department of Aerospace Engineering, Queen's Building, AIAA Student Member.

<sup>2</sup> Reader, Department of Aerospace Engineering, Queen's Building, AIAA Member.

<sup>3</sup> Sir George White Professor of Aerospace Engineering, Department of Aerospace Engineering, Queen's Building, AIAA Member.

$Q_{ij}$	= terms of the reduced stiffness matrix, $i=j=1,2,6$
$s$	= symmetric
$t^i$	= thickness of the $i$ th skin panel
$t_p$	= ply thickness
$t_w^i$	= thickness of the $i$ th spar panel
$T$	= tension
$U_i$	= material invariants, $i=1..5$
$U_i^z$	= vertical displacement of $i$ th grid of the wing
$V_T$	= potential energy due to bending
$W_i$	= weight, $i=c,d$
$wf_i^j$	= weighting factor for lamination parameters, $i=1,2,3; j=A,D$
$W_T$	= work done by the external loads
$\bar{x}, x$	= vector of design variables, abscise
$\bar{y}, y$	= gene, ordinate
$\alpha$	= angle of attack
$\varepsilon_i^{0j}$	= applied strain, $i=T,C; j=x,y,xy$
$\varepsilon_{ai}^j$	= allowable strain, $i=T,C; j=x,y,xy$
$\kappa$	= middle-surface curvatures
$\lambda_i$	= buckling or strength load factor, $i=b,s$
$\lambda^{cr}$	= critical buckling load factor
$\lambda_i^j$	= strength load factor, $i=T,C; j=x,y,xy$
$\nu_i$	= Poisson's ration in $i$ direction, $i=1,2,1$
$\xi_i^j \Big _k$	= lamination parameters for the $k$ th panel, $i=1,2,3; j=A,D$
$\rho$	= density
$\varphi$	= fibre orientation angle
$\theta$	= encoded ply angle for the skin wing-box panels
$w$	= out-of-plane displacement
$\Phi$	= swept angle

## I. Introduction

The aerospace industry is increasingly exploring the use of morphing concepts to enhance aircraft performance and adaptability<sup>1</sup>. Morphing features such as adaptability to specific flight condition or mission segments could bring major benefits. For example, an aircraft wing that adapts itself to an optimum or nearly optimum configuration, reducing drag while maintaining lift effectiveness during flight, could improve fuel consumption and increase range. Aeroelastic tailoring<sup>2-9</sup> alone or combined with structural optimisation allows structures to be designed more efficiently to meet structural or aircraft performance requirements<sup>10</sup>. However, the design of such morphing concepts requires the consideration of aerodynamic-structure coupling<sup>11-16</sup>, within the design loop.

Morphing designs can also benefit from the use of composite materials. Composite materials have the potential to be stiffness tailored, which fits in well with the purpose of aeroelastic tailoring. Composites can show anisotropic properties or elastic coupling terms. Two common types of anisotropy are membrane and flexural. Membrane and flexural anisotropy are mainly related to unbalanced or off axis laminates. Flexural anisotropy is influenced by the laminate stacking sequence, whereas membrane anisotropy is affected by the laminate volume fractions or ply percentages content. For instance, if flexural anisotropy is neglected in buckling analysis, buckling load factors can be unconservative<sup>17-18</sup>. Designing for elastic tailoring is characterised by the use of the composite anisotropy to improve composite structural performance<sup>19-21</sup>. For example, a composite plate with flexural anisotropy (that is bend-twist coupling terms) under bending loads will twist. References 22-25 provide a set of guidelines to design composite wings or flaps with bend-twist coupling. However, due to practical, manufacturing considerations, composites have been restricted to symmetric or mid-plane symmetric laminates with 0, 90, 45 and -45 degree ply angles.

Over the years, local and global optimisation techniques have been developed for composite design<sup>26-40</sup>. Local optimisations have concentrated on the specific components or part subassemblies of an aircraft structure<sup>26-38</sup> made mainly of laminated composites. Gradient (e.g. Ref. 31), GA (e.g. Ref. 34) or Gradient-GA (e.g. Ref. 35) based techniques have been developed. Composite materials have been modelled and characterised by its stacking sequence or alternatively by lamination parameters<sup>28-29</sup>. On the other hand, global optimisations have addressed the wing as a whole accounting for the interaction between components. Several methods have been proposed from single to multilevel approach, accounting for aero-structure interaction having high fidelity models (e.g. Ref. 12), characterising the wing as a beam and approximating the aerodynamics (e.g. Ref. 16), and so on. However, existing studies have limited use of aero-structure coupling, practical design rules, anisotropy in the laminated composites and structural sizing constraints.

The aim of this paper is to provide a method to design an aircraft wing of laminated composites that possesses morphing capabilities employing aeroelastic tailoring. Morphing capabilities are achieved by passive actuation. That implies that the aircraft wing will adapt itself to improve its performance during the designed flight conditions. The approach consists of an aeroelastic steady-state scheme with aero-structure coupling embedded within a global optimisation. The global optimisation is divided into two levels. At the first level, MP is used to optimise the wing under structural and aerodynamic constraints. The wing-box panels (skins and spars) are modelled using lamination parameters accounting for their anisotropy. The panels are assumed to be symmetric or mid-plane symmetric laminates with 0, 90, 45 or -45 degree ply angles. Each of the wing-box panels is subjected to a combined in-plane loading under strength, buckling and practical design constraints. At the second level, the actual lay-ups of the wing-box panels are obtained using a GA, accounting for manufacture and design practices. The novelty of the present work lies in: the use of an aeroelastic steady-state scheme with aero-structure coupling embedded within a two level global optimisation, which accounts for composite material anisotropy, lift and induced drag variations as well as internal load redistribution under structural and aerodynamic constraints.

## II. Wing geometry, structure and component loading

A swept back wing configuration as shown in Fig. 1 is considered. The wing structure is divided into the Wing-Box (WB), the Leading and Trailing Edge (LE & TE) and the ribs. The wing-box structure comprises the skin (top and bottom) and the spars (front and rear). Each of these substructures consists of several components or unstiffened panels. This study concentrates on the wing-box structure which has a predetermined layout. The wing-box is assumed to be subdivided into five rib bays, with the skin and spar panels having different properties in each bay. The skin and spar panels, due to aerodynamic forces, experience a combined loading; however it is assumed that this loading will be mainly membrane in nature. For analysis purposes and simplicity, it is also assumed that the skin and spar panels are flat and can be represented as rectangular plates with simply supported conditions along the interface with the adjacent panels. Figure 3 shows the material axis and positive sign convention for the applied loading for each of the wing-box panels.

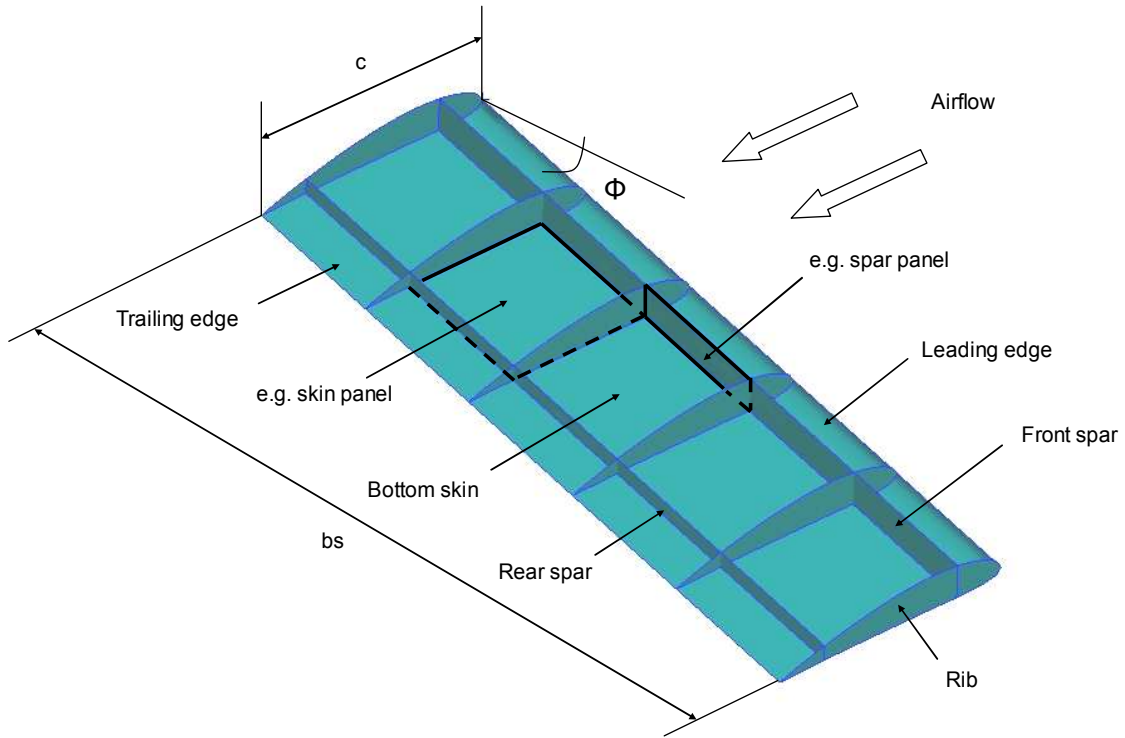


**Figure 1. Wing structure.**

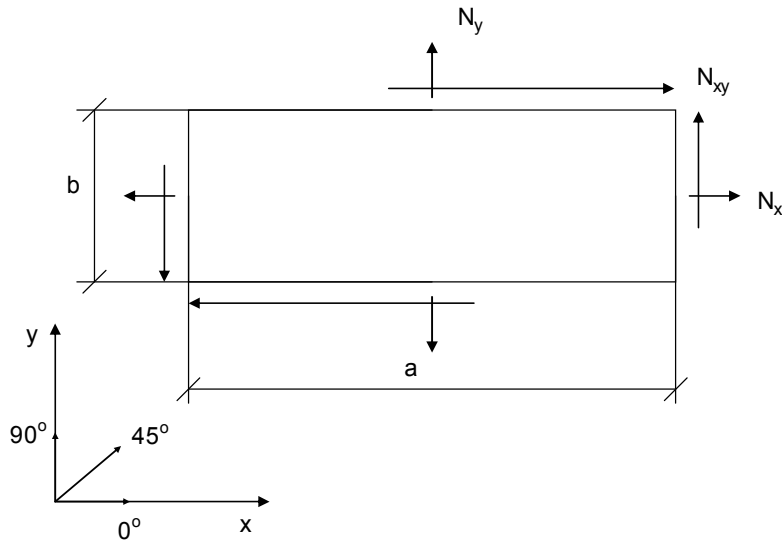


**Figure 2. Wing-box panel geometry and loading.**

### III. Aerodynamic loading

An aeroelastic steady-state response technique as shown in Fig. 3 is employed to calculate the aerodynamic loads. From initial flight conditions and wing geometry an aerodynamic mesh is produced. PANAIR<sup>41</sup> is then used to compute the aerodynamic pressure loads. The aerodynamic pressure loads are subsequently converted into nodal loads to be applied to an FE model. The structural and aerodynamic meshes share the same characteristics. The material properties together with the structural mesh and nodal loads are used to generate the FE model of the wing. FE analysis is then carried out using MD NASTRAN<sup>42</sup> to obtain the structure deformation. Figure 4 shows the FE mesh with the boundary conditions for the wing structure. Displacements at the grid positions are registered. The scheme is iterative and for each iteration the geometric distance of the grid positions is evaluated. The process

terminates when the difference of the geometric distance between iterations is less than a specified tolerance. A relaxation factor is used to achieve numerical stability.

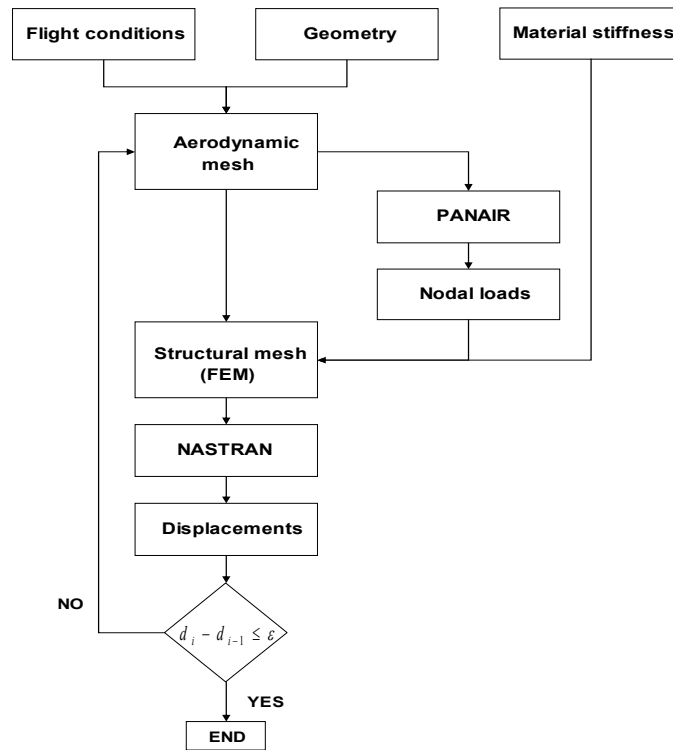


Figure 3. Aeroelastic steady-state response scheme.

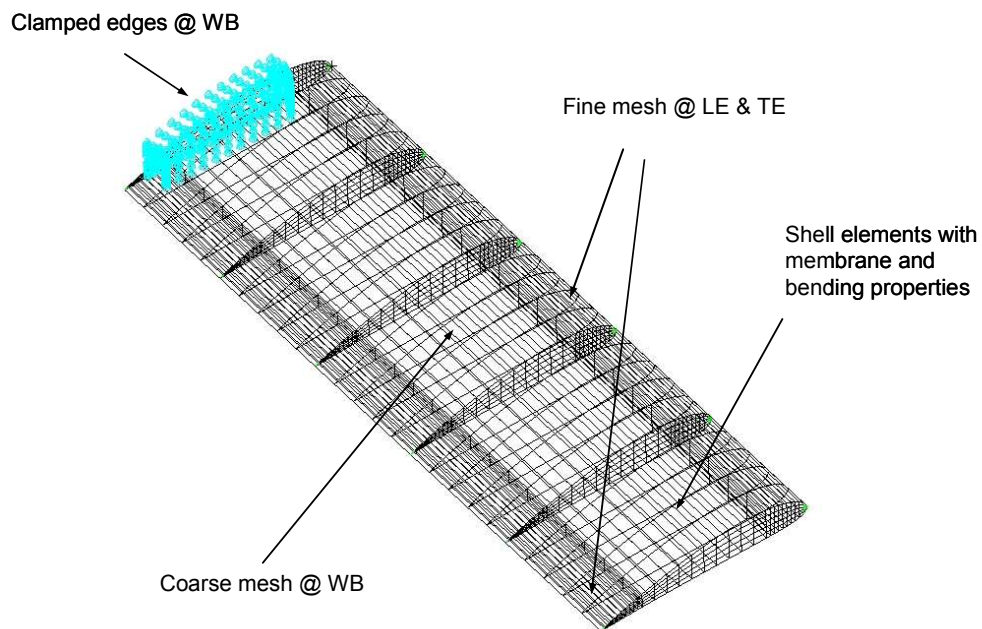


Figure 4. FE model and boundary conditions of the wing structure.

#### IV. Laminate constitutive equations

The Classical Laminate Theory (CLT)<sup>43</sup> is applied to the wing-box panels (skins and spars) assuming laminates are symmetric or mid-plane symmetric. Thus,

$$\begin{bmatrix} N \\ M \end{bmatrix} = \begin{bmatrix} A & 0 \\ 0 & D \end{bmatrix} \cdot \begin{bmatrix} \varepsilon^0 \\ \kappa \end{bmatrix} \quad (1)$$

The membrane and bending stiffness properties can be expressed in terms of material stiffness invariants ( $U$ ) and eight lamination parameters ( $\xi$ ) (e.g. Ref. 30). In addition, plies are considered orthotropic and laminated with fibre angles restricted to 0, 90, 45, and -45 degrees. As a result, lamination parameters are further reduced to six. The membrane and bending stiffnesses are determined by,

$$\begin{bmatrix} A_{11} \\ A_{12} \\ A_{22} \\ A_{66} \\ A_{16} \\ A_{26} \end{bmatrix} = h \cdot \begin{bmatrix} 1 & \xi_1^A & \xi_2^A & 0 & 0 \\ 0 & 0 & -\xi_2^A & 1 & 0 \\ 1 & -\xi_1^A & \xi_2^A & 0 & 0 \\ 0 & 0 & -\xi_2^A & 0 & 1 \\ 0 & \frac{\xi_3^A}{2} & 0 & 0 & 0 \\ 0 & \frac{\xi_3^A}{2} & 0 & 0 & 0 \end{bmatrix} \cdot \begin{bmatrix} U_1 \\ U_2 \\ U_3 \\ U_4 \\ U_5 \end{bmatrix} \quad (2)$$

$$\begin{bmatrix} D_{11} \\ D_{12} \\ D_{22} \\ D_{66} \\ D_{16} \\ D_{26} \end{bmatrix} = \frac{h^3}{12} \cdot \begin{bmatrix} 1 & \xi_1^D & \xi_2^D & 0 & 0 \\ 0 & 0 & -\xi_2^D & 1 & 0 \\ 1 & -\xi_1^D & \xi_2^D & 0 & 0 \\ 0 & 0 & -\xi_2^D & 0 & 1 \\ 0 & \frac{\xi_3^D}{2} & 0 & 0 & 0 \\ 0 & \frac{\xi_3^D}{2} & 0 & 0 & 0 \end{bmatrix} \cdot \begin{bmatrix} U_1 \\ U_2 \\ U_3 \\ U_4 \\ U_5 \end{bmatrix} \quad (3)$$

The material stiffness invariants ( $U$ ) are given as follows,

$$\begin{bmatrix} U_1 \\ U_2 \\ U_3 \\ U_4 \\ U_5 \end{bmatrix} = \frac{1}{8} \cdot \begin{bmatrix} 3 & 2 & 3 & 4 \\ 4 & 0 & -4 & 0 \\ 1 & -2 & 1 & -4 \\ 1 & -6 & 1 & -4 \\ 1 & -2 & 1 & 4 \end{bmatrix} \cdot \begin{bmatrix} Q_{11} \\ Q_{12} \\ Q_{22} \\ Q_{66} \end{bmatrix} \quad (4)$$

Additionally, the ply stiffness properties ( $Q$ ) are obtained by the following equations,

$$Q_{11} = \frac{E_{11}}{1 - \nu_{12} \cdot \nu_{21}} \quad (5)$$

$$Q_{12} = \frac{\nu_{12} \cdot E_{22}}{1 - \nu_{12} \cdot \nu_{21}} \quad (6)$$

$$Q_{22} = \frac{E_{22}}{1 - \nu_{12} \cdot \nu_{21}} \quad (7)$$

$$Q_{21} = Q_{12} \quad (8)$$

$$Q_{66} = G_{12} \quad (9)$$

$$\nu_{21} = \nu_{12} \cdot \frac{E_{22}}{E_{11}} \quad (10)$$

The membrane and bending lamination parameters are calculated, by the following integrals,

$$\xi_{[1 \ 2 \ 3]}^A = \frac{1}{h} \cdot \int_{-h/2}^{h/2} [\cos 2\varphi \ \cos 4\varphi \ \sin 2\varphi] \cdot dz \quad (11)$$

$$\xi_{[1 \ 2 \ 3]}^D = \frac{12}{h^3} \cdot \int_{-h/2}^{h/2} [\cos 2\varphi \ \cos 4\varphi \ \sin 2\varphi] \cdot z^2 \cdot dz \quad (12)$$

## V. Global optimisation strategy

The global optimisation strategy is shown as a flow chart in Fig. 4. It is divided into two stages similar to that in Ref. 21. At the first stage, the wing-box panels are optimised using lamination parameters and gradient based techniques under structural and aerodynamic constraints. The optimum thicknesses and values of the lamination parameters for each of the panels are identified. At the second stage, a GA is used to target the optimum lamination parameters to obtain the actual lay-ups for each of the skin and spar panels.

### A. First level-Gradient based optimisation

At this level a non-linear constrained optimisation is carried out employing MATLAB<sup>44</sup>. The mathematical optimisation problem is stated as follows,

Minimise	$M(\bar{x})$	Objective function
Subject to	$G_j(\bar{x}) \leq 0 \quad j = 1, \dots, n_G$	Structural inequality constraints
	$G_L(\bar{x}) \leq 0 ; G_D(\bar{x}) \leq 0$	Aerodynamic inequality constraints
	$\bar{x}^l \leq \bar{x} \leq \bar{x}^u$	Side constraints

(13)

The objective function is the mass of the wing-box panels (skins and spars), the inequality constraints consist of structural constraints such as strength, buckling or practical design rules, and aerodynamic constraints (lift and induced drag). The design variables are the thicknesses and the membrane and bending lamination parameters of the skin and spar panels. Note that for every optimisation cycle at this level, an aeroelastic-steady state scheme is performed.

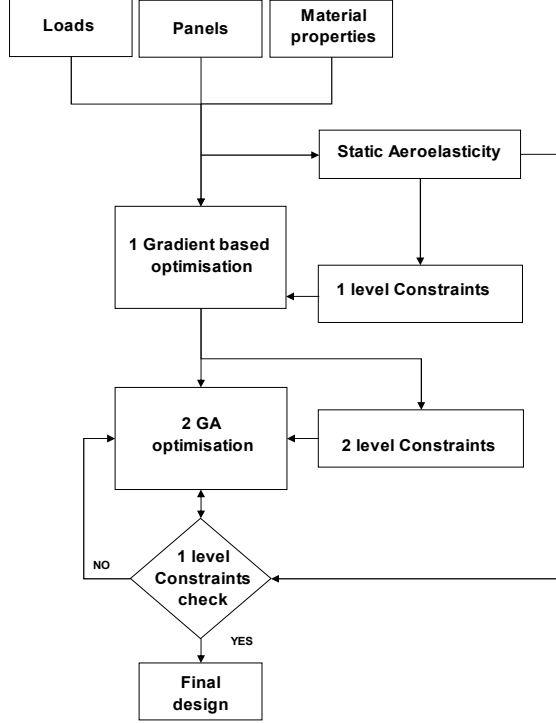


**Figure 5. Global optimisation flow chart.**

*1. Objective function*

The objective function is the sum of the weight of each of the skin and spar panels that comprises the wing-box structure. Thus,

$$M(\bar{x}) = \sum_{i=1}^n a_i \cdot (\rho_i \cdot A^i(\bar{x})) \quad (14)$$

where  $n$  denotes the total number of wing-box panels. The expressions for the skin and spar areas are as follows,

$$A_{skin}^i = t^i \cdot b^i \quad (15)$$

$$A_{spar}^i = t_w^i \cdot h_w^i \quad (16)$$

*2. Design variables*

The design variables for each of the skin and spar panels are shown in Table 1. As the wing-box is divided into five rib bays and each of the rib bays consists of four panels with seven design variables, the total number of design variables is 140.

**Table 1. Design variables of the  $i$ th wing-box panel.**

$i$ th panel	Design variables		
	$\bar{x}_i$		
	$h_i$	$\xi_{[1 \ 2 \ 3]}^A _i$	$\xi_{[1 \ 2 \ 3]}^D _i$



### 3. Design constraints

Four sets of design constraints are considered in the optimisation. The following sections describe those constraints in detail.

#### 1) Lamination parameter feasible region

The lamination parameter feasible region is extracted from Ref. 21. Thus,

$$2 \cdot \left| \xi_1^{A,D} \right| - \xi_2^{A,D} - 1 \leq 0 \quad (17)$$

$$2 \cdot \left| \xi_3^{A,D} \right| + \xi_2^{A,D} - 1 \leq 0 \quad (18)$$

$$\left( \xi_i^A - 1 \right)^4 - 4 \cdot \left( \xi_i^D - 1 \right) \cdot \left( \xi_i^A - 1 \right) \leq 0 \quad i = 1, 2, 3 \quad (19)$$

$$\left( \xi_i^A + 1 \right)^4 - 4 \cdot \left( \xi_i^D + 1 \right) \cdot \left( \xi_i^A + 1 \right) \leq 0 \quad i = 1, 2, 3 \quad (20)$$

$$\left( 2 \cdot \xi_1^A - \xi_2^A - 1 \right)^4 - 16 \cdot \left( 2 \cdot \xi_1^D - \xi_2^D - 1 \right) \cdot \left( 2 \cdot \xi_1^A - \xi_2^A - 1 \right) \leq 0 \quad (21)$$

$$\left( 2 \cdot \xi_1^A + \xi_2^A + 1 \right)^4 - 16 \cdot \left( 2 \cdot \xi_1^D + \xi_2^D + 1 \right) \cdot \left( 2 \cdot \xi_1^A + \xi_2^A + 1 \right) \leq 0 \quad (22)$$

$$\left( 2 \cdot \xi_1^A - \xi_2^A + 3 \right)^4 - 16 \cdot \left( 2 \cdot \xi_1^D - \xi_2^D + 3 \right) \cdot \left( 2 \cdot \xi_1^A - \xi_2^A + 3 \right) \leq 0 \quad (23)$$

$$\left( 2 \cdot \xi_1^A + \xi_2^A - 3 \right)^4 - 16 \cdot \left( 2 \cdot \xi_1^D + \xi_2^D - 3 \right) \cdot \left( 2 \cdot \xi_1^A + \xi_2^A - 3 \right) \leq 0 \quad (24)$$

$$\left( 2 \cdot \xi_3^A - \xi_2^A + 1 \right)^4 - 16 \cdot \left( 2 \cdot \xi_3^D - \xi_2^D + 1 \right) \cdot \left( 2 \cdot \xi_3^A - \xi_2^A + 1 \right) \leq 0 \quad (25)$$

$$\left( 2 \cdot \xi_3^A + \xi_2^A - 1 \right)^4 - 16 \cdot \left( 2 \cdot \xi_3^D + \xi_2^D - 1 \right) \cdot \left( 2 \cdot \xi_3^A + \xi_2^A - 1 \right) \leq 0 \quad (26)$$

$$\left( 2 \cdot \xi_3^A - \xi_2^A - 3 \right)^4 - 16 \cdot \left( 2 \cdot \xi_3^D - \xi_2^D - 3 \right) \cdot \left( 2 \cdot \xi_3^A - \xi_2^A - 3 \right) \leq 0 \quad (27)$$

$$\left( 2 \cdot \xi_3^A + \xi_2^A + 3 \right)^4 - 16 \cdot \left( 2 \cdot \xi_3^D + \xi_2^D + 3 \right) \cdot \left( 2 \cdot \xi_3^A + \xi_2^A + 3 \right) \leq 0 \quad (28)$$

$$\left( \xi_1^A - \xi_3^A - 1 \right)^4 - 4 \cdot \left( \xi_1^D - \xi_3^D - 1 \right) \cdot \left( \xi_1^A - \xi_3^A - 1 \right) \leq 0 \quad (29)$$

$$\left( \xi_1^A + \xi_3^A + 1 \right)^4 - 4 \cdot \left( \xi_1^D + \xi_3^D + 1 \right) \cdot \left( \xi_1^A + \xi_3^A + 1 \right) \leq 0 \quad (30)$$

$$\left( \xi_1^A - \xi_3^A + 1 \right)^4 - 4 \cdot \left( \xi_1^D - \xi_3^D + 1 \right) \cdot \left( \xi_1^A - \xi_3^A + 1 \right) \leq 0 \quad (31)$$

$$\left( \xi_1^A + \xi_3^A - 1 \right)^4 - 4 \cdot \left( \xi_1^D + \xi_3^D - 1 \right) \cdot \left( \xi_1^A + \xi_3^A - 1 \right) \leq 0 \quad (32)$$

The above constraints are imposed on each of the skin and spar panels. Further details on these constraints can be found in Ref. 38

#### 2) Strength constraints

The magnitude of the strain taken by the laminate, in tension, compression and shear in  $x$ ,  $y$  and  $xy$  directions, respectively, is limited by an allowable strain value. Laminate strains for the skin and spar panels are calculated employing CLT. Therefore,

$$\begin{bmatrix} \varepsilon_x^0 \\ \varepsilon_y^0 \\ \varepsilon_{xy}^0 \end{bmatrix} = \begin{bmatrix} A_{11} & A_{12} & A_{16} \\ A_{12} & A_{22} & A_{26} \\ A_{16} & A_{26} & A_{66} \end{bmatrix}^{-1} \begin{bmatrix} N_x \\ N_y \\ N_{xy} \end{bmatrix} \quad (33)$$

The laminate strength load factor is given by the ratio between the allowable and applied strain. Hence,

$$\lambda_i^j = \frac{\varepsilon_{ai}^j}{\varepsilon_i^{0j}} \quad i = x, y, xy; \quad j = T, C \quad (34)$$

where  $T$  and  $C$  denote tension and compression, respectively.

The failure strength at laminate level, for both the tension and compression cases, is implemented as constraints as follows,

$$\frac{1}{\lambda_i^j} - 1 \leq 0 \quad i = x, y, xy; \quad j = T, C \quad (35)$$

These constraints are applied to each of the skin and spar panels respectively.

### 3) Buckling constraints

Local buckling analysis is carried out in each of the wing-box panels. Each panel is assumed to be flat and simply supported at the interface with adjacent panels. The Rayleigh-Ritz (RR) method<sup>45</sup> is used to perform the local buckling analysis. The RR method is based on the principle of minimum potential energy. The potential energy of a system at equilibrium has an extremal value<sup>46</sup>. For the neutral equilibrium the potential energy due to bending ( $V_T$ ) is balanced by a factor ( $\lambda$ ) of the work done by the external loads ( $W_T$ ). Hence,

$$V_T - \lambda \cdot W_T = 0 \quad (36)$$

The potential energy due to bending is given by,

$$V_T = \frac{1}{2} \cdot \iint_{Area} \left[ D_{11} \frac{\partial^2 w}{\partial x^2} \frac{\partial^2 w}{\partial x^2} + 2D_{12} \frac{\partial^2 w}{\partial x^2} \frac{\partial^2 w}{\partial y^2} + D_{22} \frac{\partial^2 w}{\partial y^2} \frac{\partial^2 w}{\partial y^2} + 4 \frac{\partial^2 w}{\partial x \partial y} \left( D_{26} \frac{\partial^2 w}{\partial y^2} + D_{16} \frac{\partial^2 w}{\partial x^2} + D_{66} \frac{\partial^2 w}{\partial x \partial y} \right) \right] \cdot dy \cdot dx \quad (37)$$

The work done by the external loads is given by,

$$W_T = -\frac{1}{2} \cdot \iint_{Area} \left[ N_x \left( \frac{\partial w}{\partial x} \right)^2 + N_y \left( \frac{\partial w}{\partial y} \right)^2 + 2 \cdot N_{xy} \cdot \frac{\partial w}{\partial x} \cdot \frac{\partial w}{\partial y} \right] \cdot dy \cdot dx \quad (38)$$

For the solution procedure, the out-of-plane displacement shape is represented by a double sine Fourier series, since it satisfies the simply supported boundary conditions at the edges. Thus,

$$w(x, y) = \sum_i^m \sum_j^n A_{mn} \sin\left(\frac{m\pi x}{a}\right) \cdot \sin\left(\frac{n\pi y}{b}\right) \quad (39)$$

where  $A_{mn}$  are undetermined coefficients.

The critical buckling load is given by the lowest value or critical factor ( $\lambda^{cr}$ ), which is obtained by minimizing Eq. (36) with respect to the  $A_{mn}$  coefficients. Hence,

$$\frac{\partial}{\partial A_{mn}} (V_T - \lambda \cdot W_T) = 0 \quad (40)$$

This provides an eigenvalue problem in  $\lambda$ . The smallest non-zero solution is the critical factor. Therefore, the critical buckling load is given by,

$$\begin{bmatrix} N_x^{cr} \\ N_y^{cr} \\ N_{xy}^{cr} \end{bmatrix} = \lambda^{cr} \cdot \begin{bmatrix} N_x \\ N_y \\ N_{xy} \end{bmatrix} \quad (41)$$

Once the critical buckling factor is identified, the buckling constraint is expressed as,

$$1 - \lambda^{cr} \leq 0 \quad (42)$$

This constraint is applied individually to each of the skin and spar panels.

#### 4) Practical design constraints – Percentages of ply angles

At least 10% of each ply angle should be provided<sup>47</sup>. The maximum and minimum percentages of the ply angles for the wing-box panels, are limited. The percentages of the 0, 90, 45, and -45 degree ply angles for each of those elements are,

$$p_i = \frac{2 \cdot t_i}{h} \cdot 100 \quad i = 0, 90, 45, -45; \quad h = t, t_{sf}, t_{sw} \quad (43)$$

The design constraints imposed for the maximum and minimum percentages of the 0, 90, 45, and -45 degree ply angles, are as follows,

$$1 - \frac{p_i^{\max}}{p_i} \leq 0 \quad (44)$$

$$\frac{p_i^{\min}}{p_i} - 1 \leq 0 \quad (45)$$

#### 4. Sensitivities

Structural sensitivities are determined by the chain rule differentiation<sup>48</sup> as shown in Eq. (46). This is required because the structural sensitivities are a function of the internal loads and the internal loads themselves are a function of the design variables. Design sensitivity and optimisation solution (SOL 200) of MD NASTRAN<sup>49</sup> and a global FE model are employed to obtain the sensitivity of the internal loads with respect to the design variables.

$$\frac{\partial G_i(\bar{x})}{\partial x_j} = \frac{\partial G_i(\bar{x})}{\partial x_j} + \frac{\partial G_i(\bar{N})}{\partial N_k} \cdot \frac{\partial N_k(\bar{x})}{\partial x_j} \quad (46)$$

Sensitivities of the constraints with respect to both design variables and internal loads are calculated by the forward finite difference approximation given by,

$$\frac{\partial G_i(\bar{x})}{\partial X_j} = \frac{G_i(\bar{x} + \Delta x_j) - G_i(\bar{x})}{\Delta X_j} \quad X = x, N \quad (47)$$

where  $\Delta X_j$  is a small perturbation times the  $j$ th design variable or internal load. A suitable perturbation step size was determined to be 0.0001 after a trial and error exercise.

Moreover, aerodynamic sensitivities are also calculated employing the chain rule. They are determined assuming that a small rotation around the leading edge produces a variation in the lift, induced drag and vertical displacements. Thus,

$$\frac{\partial G_k(\bar{x})}{\partial x_j} = \frac{\partial G_k(\bar{x})}{\partial \theta_j} \cdot \frac{\Delta \theta_j}{\partial U_j^z} \cdot \frac{\partial U_j^z}{\partial x_j} \quad k = L, D \quad (48)$$

where  $\Delta \theta_j$  is a small rotational perturbation. A trial and error process was performed and a suitable step size for the perturbation was determined to be 0.05. The vertical displacements are computed at the grids in the interface with the skins, the leading and trailing edge. Note, that the second and third terms of Eq. (48) are calculated analytically and using SOL 200 in MD NASTRAN, respectively.

#### B. Second level-GA based optimisation

A standard GA<sup>50-51</sup> is employed at this level to solve the discrete lay-up optimisation problem. The lamination parameters from the first optimisation level are targeted to obtain the actual lay-ups for the skin and spar panels. A typical GA structure consists of generation of population, evaluation, elitism, crossover, reproduction and mutation. Note that at this level the GA is applied separately to each of the wing-box panels.

#### 5. Fitness function

The fitness function is expressed in terms of the square difference between the optimum and targeted lamination parameters<sup>38</sup> plus extra penalty terms to account for ply contiguity constraints<sup>21</sup>. Thus,

$$f(\bar{y}) = \sum_{i=1}^3 w f_i^A \cdot (\xi_i^A - \xi_{iopt}^A)^2 + \sum_{i=1}^3 w f_i^D \cdot (\xi_i^D - \xi_{iopt}^D)^2 + \sum_{k=1}^4 \Theta_k \quad (49)$$

where  $\bar{y}$  is the design variable vector or gene representing the laminate stacking sequence,  $wf_i^{A,D}$  are weighting factors and  $\Theta_k$  are the penalty functions terms to limit the number of plies of the same orientation stacked together. When more than 4 plies of the same orientation are stacked together<sup>32</sup> the value of  $\Theta_k$  is 1 otherwise it is 0.

### 6. Genes

The design variables are the thicknesses and the 0, 90, 45, and  $-45$  degree ply angles that constitute the laminate stacking sequences for the wing-box panels. These variables are modelled as chromosomes in genes within the GA. The corresponding encoded chromosomes to ply angles are: 1, 2, 3, 4, 5, 6 and 7 for  $\pm 45, 90, 0, 45, -45, 90, 0$ , degrees, respectively. Figure 6 shows the modelling of the gene for a panel. The panel thickness is given by  $h$ , the encoded ply angle is  $\theta$  and  $n$  corresponds to half or half plus one plies depending on whether the panel laminate is symmetric or mid-plane symmetric.

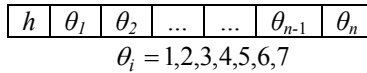


**Figure 6. Gene with chromosomes for a wing-box panel.**

## VI. Numerical examples

A typical UAV aircraft with a swept back wing configuration is used to test the two level approach herein presented. For the flight case, which constitutes the up-bending case, it is assumed that the aircraft is flying at 5000 m, with a speed of 100 m/s, and angle of attack ( $\alpha$ ) of 8 degrees. The load factor is assumed to be 2.5 representing a manoeuvre case. For sizing purposes an up-bending case and a down-bending (70% of up-bending) case were considered. The airfoil used is NACA 4412. The wing has a swept back angle of 15 degrees. The wing chord and semi-span are 400 and 1200 mm, respectively. The front and rear spars are located at 20% and 80% of the wing chord, respectively. The wing-box is made of P100/AS3501 with the following properties:  $E_{11} = 369000 \text{ N/mm}^2$ ,  $E_{22} = 5030 \text{ N/mm}^2$ ,  $\nu_{12} = 0.31$ ,  $G_{12} = 5240 \text{ N/mm}^2$ ,  $t_p = 0.125 \text{ mm}$  and  $\rho = 1.6 \cdot 10^{-6} \text{ kg/mm}^3$ . The leading and trailing edges as well as the ribs are made of an aluminium alloy with the following properties:  $E = 72000 \text{ N/mm}^2$ ,  $G = 26900 \text{ N/mm}^2$ ,  $\nu = 0.3$  and  $\rho = 2.7 \cdot 10^{-6} \text{ kg/mm}^3$ . The thicknesses of the leading and trailing edges for the 5 rib bays starting at the wing root are: 2, 1.75, 1.5, 1 and 0.875 mm, respectively. Each of the ribs has a thickness of 0.25 mm.

Firstly, the two level optimisation approach was performed with structural constraints and without aerodynamic constraints (i.e. lift and induced drag were not restricted). The structural constraints were: strength, buckling, practical design and ply contiguity constraints. At the first level, a minimum thickness for the skin and spar panels was set as 0.875 mm. The minimum percentage of each ply angle was limited to 10%. Strength constraints were applied to limit the strains in  $x$ ,  $y$  and  $xy$  directions in both tension and compression to  $3600\mu\epsilon$ ,  $3600\mu\epsilon$ , and  $7200\mu\epsilon$ , respectively. 49 terms ( $m = n = 7$ ) were used in the double sine series for the RR method. At the second level, a GA code was used with a population of 40, 200 generations, a 0.7 probability of crossover and a 0.05 probability of mutation as well as assuming that all weighting factors for the lamination parameters were equal to 1 and locating at least one set of  $\pm 45$  degree plies at the outer surface of the laminates. Table 1 contains the total weight (wing-box, leading and trailing edge and ribs) of the wing for the continuous ( $W_c$ ) and discrete ( $W_d$ ) levels as well as the final lift and induced drag. Table 2 details the optimum design obtained. Figure 7 shows the displacement of the optimum wing for the up-bending case.

**Table 2. Total weights, lift and induced drag for optimum design wing with structural constraints.**

$W_c / W_d$ [Kg]	$L$ [N]	$D$ [N]
3.51/3.59	3151.6	181.2

**Table 3. Optimum skin and spar panels for a wing under structural constraints.**

Top skin				
RBN	$\lambda_b$	$\lambda_s$	Lay-up	0%/45%/-45%/90%
1	1.05	4.07	$[(\pm 45)_2/-45/(\pm 45)_3/90/0/90]_{MS}$	8/37/44/11
2	1.03	4.42	$[\pm 45/-45/45/(\pm 45)_2/0/90]_{MS}$	10/40/40/10
3	1.25	7.51	$[\pm 45/-45/45_2/-45/90/0/-45]_{MS}$	12/35/41/12
4	1.51	12.91	$[(\pm 45)_2/-45/90/0]_{MS}$	8/31/46/15
5	1.57	11.43	$[\pm 45/90/0]_{MS}$	14/29/29/28
Bottom skin				
RBN	$\lambda_b$	$\lambda_s$	Lay-up	0%/45%/-45%/90%
1	1.11	4.22	$[\pm 45/-45/(\pm 45)_3/45/0/90/90]_{MS}$	8/40/40/12
2	1.07	7.16	$[(\pm 45)_3/90/0/-45]_{MS}$	12/35/41/12
3	1.15	10.17	$[\pm 45/45/\pm 45/90/0]_{MS}$	8/46/31/15
4	1.58	-	$[(\pm 45)_2/90/0]_{MS}$	9/36/36/18
5	2.73	11.43	$[\pm 45/90/0]_{MS}$	14/29/29/28
Front spar				
RBN	$\lambda_b$	$\lambda_s$	Lay-up	0%/±45%/90%
1	1.48	3.09	$[\pm 45/90/0]_{MS}$	14/58/28
2	3.80	6.32	$[\pm 45/90/0]_{MS}$	14/58/28
3	5.54	9.20	$[\pm 45/90/0]_{MS}$	14/58/28
4	10.76	10.04	$[\pm 45/90/0]_{MS}$	14/58/28
5	-	-	$[\pm 45/90/0]_{MS}$	14/58/28
Rear spar				
RBN	$\lambda_b$	$\lambda_s$	Lay-up	0%/±45%/90%
1	8.79	4.15	$[\pm 45/90/0]_{MS}$	14/58/28
2	-	13.05	$[\pm 45/90/0]_{MS}$	14/58/28
3	-	17.11	$[\pm 45/90/0]_{MS}$	14/58/28
4	-	-	$[\pm 45/90/0]_{MS}$	14/58/28
5	-	-	$[\pm 45/90/0]_{MS}$	14/58/28

Note that the buckling load factors provided in Table 3 for the top and bottom skins correspond to the up and down bending case respectively. In case of the spars, the buckling load factors given are the lowest of the up-and down bending cases. Strength load factors for both the skin and spar panels are the lowest covering the tension and compression cases. Load factors greater than twenty are not shown. Assessing the load factors, it is clearly seen that the optimum design is driven by buckling. It is observed that some panels have high buckling load factors. This is as a result of imposing the minimum skin thickness constraint. It is also observed that the skins do not exhibit much membrane and flexural anisotropy. This is because longitudinal loads drive the buckling behaviour. Note that the spars do not require thickening. Note also that some skin panels do not satisfy completely the 10% rule and do not maintain continuity in plies with their adjacent neighbours.

Next, the two level approach was applied to carry out an optimisation with the same structural constraints as above plus aerodynamic constraints. The aerodynamic constraints imposed were to have at least 99% of the lift and to have an induced drag less than the previous optimum wing design. The lift and induced drag as well as the total weight of the continuous and discrete levels of this new optimum wing design are listed in Table 4. The new optimum wing design obtained is shown in Table 5. Figure 8 shows the displacement achieved by this new optimum wing design for the up-bending case.

**Table 4. Total weights, lift and induced drag for optimum design wing with structural constraints.**

$W_c / W_d$ [Kg]	$L$ [N]	$D$ [N]
4.10/4.26	3136.3	178.6

**Table 5. Optimum skin and spar panels for a wing under structural and aerodynamic constraints.**

Top skin				
RBN	$\lambda_b$	$\lambda_s$	Lay-up	0%/45%/-45%/90%
1	1.46	4.30	$[\pm 45 / -45 / \pm 45 / 45_4 / 90 / 45_2 / 0 / 90 / 0]_{MS}$	10/55/21/14
2	2.19	4.96	$[\pm 45 / -45 / \pm 45 / 45_4 / 90_2 / 45 / 0]_S$	8/54/23/15
3	1.38	7.31	$[\pm 45 / 45_4 / 0 / 45 / 90]_S$	11/67/11/11
4	3.20	16.85	$[\pm 45 / 45_4 / 0 / 45 / 90]_S$	11/67/11/11
5	16.39	-	$[\pm 45 / 45_4 / 0 / 45 / 90]_S$	11/67/11/11
Bottom skin				
RBN	$\lambda_b$	$\lambda_s$	Lay-up	0%/45%/-45%/90%
1	1.47	4.31	$[\pm 45 / -45 / \pm 45 / 45_4 / 90_2 / 0 / 45]_S$	8/53/23/15
2	3.54	8.37	$[\pm 45 / -45 / \pm 45 / 45_3 / 90 / 45_2 / 0 / 90]_S$	8/53/23/15
3	2.29	12.18	$[\pm 45 / 45_4 / 0 / 45 / 90]_S$	11/67/11/11
4	4.86	-	$[\pm 45 / 45_4 / 0 / 45 / 90]_S$	11/67/11/11
5	-	-	$[\pm 45 / 45_4 / 90 / 45 / 0]_S$	11/67/11/11
Front spar				
RBN	$\lambda_b$	$\lambda_s$	Lay-up	0%/±45%/90%
1	1.56	3.28	$[\pm 45 / 90 / 0]_{MS}$	14/58/28
2	4.08	7.36	$[\pm 45 / 90 / 0]_{MS}$	14/58/28
3	5.92	11.05	$[\pm 45 / 90 / 0]_{MS}$	14/58/28
4	11.67	-	$[\pm 45 / 90 / 0]_{MS}$	14/58/28
5	-	-	$[\pm 45 / 90 / 0]_{MS}$	14/58/28
Rear spar				
RBN	$\lambda_b$	$\lambda_s$	Lay-up	0%/±45%/90%
1	8.43	3.85	$[\pm 45 / 90 / 0]_{MS}$	14/58/28
2	-	14.93	$[\pm 45 / 90 / 0]_{MS}$	14/58/28
3	-	-	$[\pm 45 / 90 / 0]_{MS}$	14/58/28
4	-	-	$[\pm 45 / 90 / 0]_{MS}$	14/58/28
5	-	-	$[\pm 45 / 90 / 0]_{MS}$	14/58/28

These results show a potential improvement of the wing aerodynamic performance. This performance occurs as a result of the reduction in the induced drag (approx. 1.4%) while just decreasing slightly the lift (approx. 0.5%). However, this improvement in wing performance has a weight penalty associated of approximately 18.7%. From Table 5, it is clearly seen that the skins now exhibit membrane anisotropy and flexural anisotropy, which enables wing twist and hence reduces drag. It is observed that in the areas of the wing where buckling is the critical constraint (e.g. in the skin panels at the wing root), the content of both anisotropies decrease in the panels. However, the presence of membrane and flexural anisotropy in the wing skins increases the laminate thickness. Note that the optimum wing with just structural constraints has the skin and spar panels at the tip with minimum thickness (total of 7 plies). In contrast, the new optimum wing with structural and aerodynamic constraints contains a total of 18 plies in the skin panels from rib bays 3-5. These skin laminates are largely unbalanced to provide sufficient wing twist to reduce the drag. As previously stated, note that some skin panels do not satisfy completely the 10% rule and do not maintain continuity in plies with their adjacent neighbours.

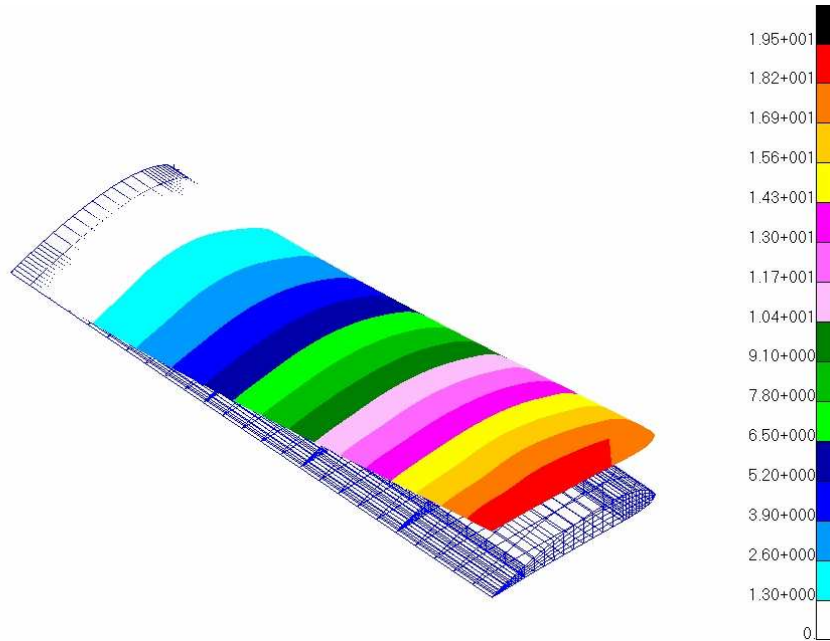


**Figure 7. Displacement of the optimised wing for the up-bending case under structural constraints. Units in mm.**

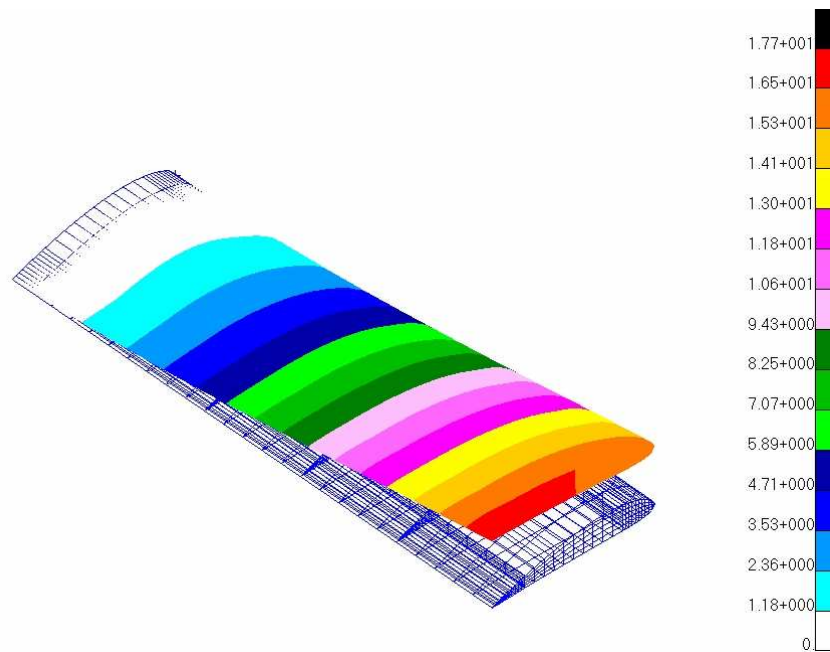


**Figure 8. Displacement of the optimised wing for the up-bending case under structural and aerodynamic constraints. Units in mm.**

From comparing the above figures, it is clearly observed that the wing of Fig. 8 shows an additional wing twist. This twist has been generated as a consequence of the membrane anisotropy of the wing-box panels (i.e. under bending loads the top skin will shear in opposite direction to the bottom skin inducing a twist moment).



## VII. Future work

Future work is planned and will include: assessing different wing configurations and structural layouts, investigating the use of response surfaces for the local panel design, evaluating different objective functions which combine weight and aerodynamic performance as well as considering lay-up continuity between adjacent panels.

## VIII. Conclusions

An approach to design an aircraft wing with morphing capabilities employing aeroelastic tailoring is presented. Morphing capabilities are achieved by passive actuation, that is the aircraft wing will modify its shape to improve flight performance. In this case, maintaining an approximate constant lift while reducing the induced drag. The approach consists of an aeroelastic steady-state scheme with aero-structure coupling embedded within a global optimisation. The global optimisation is divided into two levels. At the first level, MP is used to optimise the wing under structural and aerodynamic constraints. The wing-box panels (skins and spars) are modelled using lamination parameters accounting for their membrane and flexural anisotropy. The wing-box panels are assumed to be symmetric or mid-plane symmetric laminates with 0, 90, 45 or -45 degree ply angles. Each of the wing-box panels is subjected to a combined in-plane loading under strength, buckling and practical design constraints. At the second level, the actual lay-ups of the wing-box panels are obtained using a GA, accounting for manufacture and design practices.

For the case considered, the results have shown that a potential reduction in the induced drag (approx. 1.4%) of the wing can be achieved using laminates that contain membrane anisotropy. However, this improvement has associated a structure weight penalty of approximately 18.7%.

Overall the two level optimisation approach has performed well although slow convergence has been observed when applying aerodynamic constraints. It has also been observed that the static aeroelastic scheme tend to converge slowly when laminates contained membrane anisotropy.

## Acknowledgments

The authors thank the EC for the Marie-Curie Excellence Grant MEXT-CT-2003-002690.

## References

- <sup>1</sup> Wlezien, R. W. , Horner , G. C., McGowan, A. R., Padula, S. L., Scout, M. A., Silcox, R. J., and Simpson, J. O. "The aircraft morphing program", AIAA-1998-1927, 39th AIAA/ASME/ASCE/AHS/ASC Structures, Structural Dynamics, and Materials Conference, Long Beach, CA, 20-23 April, 1998.
- <sup>2</sup> Shirk, M. H., Hertz, T. J., and Weisshaar, T.A. "Aeroelastic tailoring-theory, practice and promise". Journal of Aircraft. Vol. 23, No. 1, pp. 6-18, 1986.
- <sup>3</sup> Haftka, R. T. "Structural optimisation with aeroelastic constraints: a survey of US applications". Int. J. of Vehicle Design. Vol. 7, nos ¾, 1986.
- <sup>4</sup> Weisshaar, T. A., and Ryan, R. J. "Control of aeroelastic instabilities through stiffness cross-coupling". Journal of Aircraft, Vol. 23, pp. 148-155, 1986.
- <sup>5</sup> Eschenauer, H. A., Schuhmacher, G., and Hartzheim, W. "Multidisciplinary design of composite aircraft structures by lagrange". Computers and Structures, Vol. 44, No. 4, pp. 877-893, 1992.
- <sup>6</sup> Popelka, D., Lindsay, D., Jr, Parham T., Berry, V., and Baker, D. J. "Results of an aeroelastic tailoring study for a composite tiltrotor wing". 51st Annual Forum of the American Helicopter Society, Forth Worth, TX, May 9-11, 1995.
- <sup>7</sup> Miura, H., Chattopadhyay, A., and Jha, R. "Development of a composite tailoring technique for airplane wing". NASA-CR-202357.
- <sup>8</sup> Gimmetstad, D. "Aeroelastic tailoring of a composite winglet for KC-135". AIAA-1981-607.
- <sup>9</sup> Eastep, F. E., Tischler, V. A., Venkayya, V. B. and Knot, N. S. "Aeroelastic tailoring of composite structures". Journal of Aircraft. Vol. 36, No. 6, pp. 1041-1047, 1999.
- <sup>10</sup> Knot, N. S., Zweber, J. V., Veley, D. E., Öz, H., and Eastep, F. E. "Flexible composite wing with internal actuation for roll maneuver". Journal of Aircraft. Vol. 39, No. 4, pp. 521-527, 2002.
- <sup>11</sup> Visser, J.A.P. "Aeroelastic and strength optimisation of a composite aircraft wing using a multilevel approach". AIAA-99-1258, 1999.
- <sup>12</sup> Reuther, J., Alonso, J. J., Martins, J. R. R. A., and Smith, S. C. "A coupled aero-structural optimisation method for complete aircraft configurations". 37<sup>th</sup> Aerospace Science Meeting and Exhibit, Reno, NV, January 11-14, 1999.
- <sup>13</sup> Gumbert, C. R., Hou, G. J. W., and Newman, P. A. "Simultaneous aerodynamic and structural design optimisation (SASDO) for a 3-D wing". AIAA-2001-2527, 15th AIAA Computational Fluid Dynamics Conference, Anaheim, California, 11-14 June, 2001.

- <sup>14</sup> Martins, J. R. R. A., Alonso, J. J., and Reuther, J. J. "High-fidelity aero-structural design optimisation of a supersonic business jet". 43<sup>rd</sup> AIAA/ASME/ASCE/AHS/ASC Structures, Structural Dynamics and Materials Conference, Denver, CO, April 22-25, 2002.
- <sup>15</sup> Maute, K., Allen, M. "Conceptual design of aeroelastic structures by topology optimisation". *Struct. Mult. Opt.*, Vol. 27, pp. 27-42, 2004.
- <sup>16</sup> Weisshaar, T. A., and Duke, D. K. "Induced drag reduction using aeroelastic tailoring with adaptive control surfaces". *Journal of Aircraft*, Vol. 43, No. 1, pp. 157-164, 2006.
- <sup>17</sup> Ashton, J. E. and Waddoups, M. E. "Analysis of anisotropic plates". *Journal of composite materials*, Vol. 3, pp. 148-165, 1969.
- <sup>18</sup> Chamis, C. C. "Buckling of anisotropic composite plates". *Journal of the structural division, Proceedings of the ASCE*. Vol. 95, ST10, pp. 2119-p2139, 1969.
- <sup>19</sup> Fukunaga, H., Sekine, H., Sato, M. and Iino, A. "Buckling design of symmetrically laminated plates using lamination parameters". *Computers and structures*, Vol. 57, No. 4, pp. 643-649, 1995.
- <sup>20</sup> Fukunaga, H. and Sekine, H. "A laminate design for elastic properties of symmetric laminates with extension-shear or bending-twisting coupling". *Journal of Comp. Mat.*, Vol. 28, No. 8, pp. 708-731, 1994.
- <sup>21</sup> Herencia, J.E, Weaver, P.M, Friswell, M.I, "Local optimisation of long anisotropic laminated fibre composite panels with T shape stiffeners". 47th AIAA/ASME/ASCE/AHS/ACS Structures, Structural Dynamics & Materials Conference, Newport, RI, 1-4 May 2006.
- <sup>22</sup> Rehfield, L. W. and Cheung, R. H. "Some basic strategies for aeroelastic tailoring of wings with bend-twist coupling: part one". AIAA 2003-2006, 44<sup>th</sup> AIAA/ASME/ASCE/AHS Structures dynamics, and materials conference, Norfolk, Virginia, 7-10 April 2003.
- <sup>23</sup> Rehfield, L. W., Cheung, R. H., and Sikola, B. "Strategies for tailoring wings with bend-twist coupling: part two". AIAA 2004-1835, 45<sup>th</sup> AIAA/ASME/ASCE/AHS Structures dynamics, and materials conference, Palm Spring, California, 19-22 April, 2004.
- <sup>24</sup> Lemanski, S. L. and Weaver, P. M. "Flap-Torsion Coupling in Prismatic Sections", 45th AIAA,ASCE,ASME,AHS SDM conference, Palm Springs, USA, 2004.
- <sup>25</sup> Lemanski, S. L. and Weaver P. M. "Flap-Torsion Coupling in Sandwich beams and filled box-sections" *Thin-Walled Structures*, Vol 43, pp. 923-955, 2005.
- <sup>26</sup> Schmit, L. A and Farshi, B. "Optimum laminate design for strength and stiffness". *Int. J. Num. Meth. in Eng.*, Vol. 7, pp. 519-536, 1973.
- <sup>27</sup> Schmit, L. A and Farshi, B. "Optimum design of laminated fibre composite plates". *Int. J. Num. Meth. in Eng*, Vol. 11, pp. 623-640, 1977.
- <sup>28</sup> Tsai, S. W., Halpin, J. C. and Pagano, N. J. "Composite materials workshop". Technomic Publishing Co., Inc., 750 Summer St., Stamford, Conn. 06902. pp. 233-253, 1968.
- <sup>29</sup> Tsai, S. W. and Hahn, H. T. "Introduction to composite materials". Technomic Publishing Co., Inc., 750 Summer St., Stamford, Conn. 06902, 1980.
- <sup>30</sup> Miki, M. and Sugiyama, Y. "Optimum design of laminated composite plates using lamination parameters". AIAA-91-0971-CP, 1991.
- <sup>31</sup> Fukunaga, H. and Vanderplaats, G. N. "Stiffness optimisation of orthotropic laminated composites using lamination parameters". *AIAA Journal*, Vol. 29, No. 4, pp. 641-646, 1991.
- <sup>32</sup> Haftka, R. T. and Walsh, J. L. "Stacking sequence optimisation for buckling of laminated plates by integer programming". *AIAA Journal*, Vol. 30, No. 3, pp. 814-819, 1992.
- <sup>33</sup> Nagendra, S., Haftka, R. T. and Gürdal, Z. "Stacking sequence optimisation of simple supported laminates with stability and strain constraints". *AIAA Journal*, Vol. 30, No. 8, pp. 2132-2137, 1992.
- <sup>34</sup> Le Riche, R. and Haftka, R. T. "Optimisation of laminate stacking sequence for buckling load maximisation by genetic algorithm". *AIAA Journal*, Vol. 31, No. 5. 1993.
- <sup>35</sup> Yamazaki, K. "Two-level optimisation technique of composite laminate panels by genetic algorithms". AIAA-96-1539-CP, 1996.
- <sup>36</sup> Autio, M. "Determining the real lay-up of a laminate corresponding to optimal lamination parameters by genetic search". *Struct. Mult. Opt.*, Vol. 20, pp. 301-310, 2000.
- <sup>37</sup> Liu, B., Haftka R. T. and Trompette P. "Maximisation of buckling loads of composite panels using flexural lamination parameters". *Struct. Mult. Opt.*, Vol. 26, pp. 28-36, 2004.
- <sup>38</sup> Diaconu, C. G. and Sekine, H. "Layup optimisation for buckling of laminated composite shells with restricted layer angles". *AIAA Journal*, Vol. 42, No. 10, pp. 2153-2163, 2004.
- <sup>39</sup> Ragon, S. A., Gürdal, Z., Haftka, R. T., and Tzong, T. J. "Bilevel design of a wing structure using response surfaces". *Journal of aircraft*. Vol. 40, No. 5. 2003.
- <sup>40</sup> Liu, B. and Haftka R. T. "Single level composite wing optimisation based on flexural lamination parameters". *Struct. Mult. Opt.*, Vol. 26, pp. 111-120, 2004.
- <sup>41</sup> Magnus, E., and Epton, M. E. "PANAIR - A computer program for predicting subsonic or supersonic linear potential flows about arbitrary configurations using a higher order panel method". NASA CR 3251, 1980.
- <sup>42</sup> MD NASTRAN 2006r1. MSC Software, 2006.
- <sup>43</sup> Jones, R. M. "Mechanics of composite materials". 2<sup>nd</sup> edition, Taylor and Francis, Inc., 325 Chestnut street, Philadelphia, PA 19106, 1999.
- <sup>44</sup> MATLAB software V.7.1. The MathWorks, Inc. 1994-2006.

- <sup>45</sup> Ashton, J. E. and Whitney, J. M. "Theory of laminated plates". Technomic Publishing Co., Inc., 750 Summer St., Stamford, Conn. 06901, 1970.
- <sup>46</sup> Lekhnitskii, S. G. "Anisotropic plates". Gordon and Breach, Science Publishers, Inc., 150 Fifth Avenue, New York, N. Y. 10011. USA, 1968.
- <sup>47</sup> Niu, C. Y. M. "Composite airframe structures-Practical design information and data". Hong Kong Conmilit Press Limited. 1992.
- <sup>48</sup> Vanderplaats, G. N. "Numerical optimisation techniques for engineering design". 3<sup>rd</sup> Ed. Vanderplaats Research & Development, Inc. 1767 S. 8<sup>th</sup> Street, Colorado Springs, CO 80906. USA, 2001.
- <sup>49</sup> MSC/NASTRAN Design sensitivity and optimisation, user's guide. 2004.
- <sup>50</sup> Gürdal, Z., Haftka, R. T. and Hajela, P. "Design optimisation of laminated composite materials". John Wiley and Sons, Inc., 1999.
- <sup>51</sup> Coley, D. A. "An introduction to genetic algorithms for scientist and engineers". World Scientific Publishing Co. Pte. Ltd., P. O. Box 128, Farrer Rd, Singapore 912805, 1999.